## *NUTM1* is a recurrent fusion gene partner in B-cell precursor acute lymphoblastic leukemia associated with increased expression of genes on chromosome band 10p12.31-12.2

For 20-25% of patients with pediatric B-cell precursor acute lymphoblastic leukemia (BCP-ALL), the driving cytogenetic aberration is unknown. Identification of the primary lesion could provide better risk stratification and even identify possible treatment options. We therefore aimed to find novel recurrent genetic aberrations in BCP-ALL cases. We identified an in-frame *SLC12A6-NUTM1* fusion, resulting in expression of 3' exons of *NUTM1*, and six additional *NUTM1*-rearranged fusion cases. These *NUTM1*-rearranged cases were associated with high expression of a cluster of genes on chromosome band 10p12.31-12.2, including the *BMI1* gene. Our data point to *NUTM1* fusions as a new entity of BCP-ALL negative for known genetic abnormalities.

Pediatric BCP-ALL consists of many cytogenetic subtypes, each with a different prognosis.[1] *ETV6-RUNX1* fusions, high hyperdiploid, and *TCF3-PBX1* fusions have a favorable prognosis, while *BCR-ABL1* fusions and *KMT2A/MLL*-rearrangements have a poor prognosis. However, 20-25% of BCP-ALL patients do not have one of these sentinel cytogenetic aberrations and are therefore said to have B-other ALL. This B-other ALL subgroup has an intermediate risk of relapse, but includes both high- and low-risk subgroups that are currently being identified. Our laboratory identified a subtype with a similar expression profile and prognosis as *BCR-ABL1*, namely *BCR-ABL1*-like, within the B-other ALL subgroup.[2] The B-other ALL subgroup also includes other rare cytogenetic subtypes, such as intrachromosomal amplification of chromosome 21 and a dicentric chromosome (9;20).[1] It is important to identify more primary lesions in the remaining B-other ALL for better risk stratification and identification of possible treatment options. In this study, we aimed to identify recurrent fusions in BCP-ALL cases without currently known lesions through RNA sequencing.

We used paired-end total RNA Illumina sequencing to detect fusion genes using STAR-fusion and FusionCatcher in a population-based ALL cohort (n=71). We compared gene expression levels in a larger population-based ALL cohort (n=661) and an infant ALL cohort (n=70) using Affymetrix U133 Plus2 expression arrays. Fluorescence *in situ* hybridization (FISH) was performed

**Table 1.** Characteristics of five pediatric and two infant *NUTM1*-rearranged cases.

| Case | Sex | Age | WBC count (x10$^9$/L) | Protocol-risk arm | Outcome (years) | BCP-ALL subtype | Karyotype | FISH result | *NUTM1* fusion | Deletions[1] | Mutations[2] |
|---|---|---|---|---|---|---|---|---|---|---|---|
| 1 (index) | M | 14 (years) | 4.1 | ALL10-SR | CCR 5.0 | *BCR-ABL1*-like | 46,XY[22] | No break apart (inversion between probes) | *SLC12A6* ex2 - *NUTM1* ex3 (RNA-seq, RT-PCR + Sanger sequencing) | Not done | *FLT3* p.Ile836del |
| 2 | M | 12 (years) | 5.4 | COALL03-HR | CCR 6.2 | B-other ALL | – | Break apart | *CUX1* ex23 - *NUTM1* ex5 (RNA-seq, RT-PCR + Sanger sequencing) | *RB1* | No mutations |
| 3 | F | 8 (years) | 6.6 | ALL10-SR | CCR 4.8 | B-other ALL | 46,XX, t(7;15)(q22;q1?3)[9]/46,XX[1] | Not done | *CUX1* ex23 - *NUTM1* ex4 (RT-PCR + Sanger sequencing) | No deletions | No mutations |
| 4 | M | 6 (years) | 34.7 | ALL9-SR | CCR 11.4 | B-other ALL | 46,XY,t(7;15)(p11.2;q15), ?t(19;19)(p13.3;q13.3)[24]/ 46,XY,idem,?t(9;16)(p21;q24)[2] | Break apart | *IKZF1* ex7 - *NUTM1* ex5 (RT-PCR + Sanger sequencing) | No deletions | No mutations |
| 5 | M | 1 (years) | 48.7 | ALL8-MR | CCR 13.8 | *BCR-ABL1*-like | – | Break apart | Suspected | *IKZF1*; *EBF1* | Not done |
| 6 | M | 6 (months) | 13.3 | Interfant-99 SR | CCR 9.3 | Non-*KMT2A* rearranged | 46,XY[32] | Not done | Suspected | Not done | Not done |
| 7 | F | 9 ( months) | 60 | Interfant-99 SR | CCR 8.3 | Non-*KMT2A* rearranged | 48,XX,-15, +22,+mar1, +mar2 | Break apart | *ACIN1* ex4 - *NUTM1* ex3 (RNA-seq) | *PAX5* | Not done |

[1]As determined by SALSA P335 version A3 ALL-IKZF1 MLPA assay (MRC-Holland), as previously described.[5] [2]Custom MiSeq panel including *RAS* and *JAK* pathway genes, as previously described[15] WBC: white blood cell; BCP-ALL: B-cell precursor acute lymphoblastic leukemia; FISH: fluorescence *in situ* hybridization; CCR, continuous complete remission; RNA-seq, RNA sequencing; ex, exon.

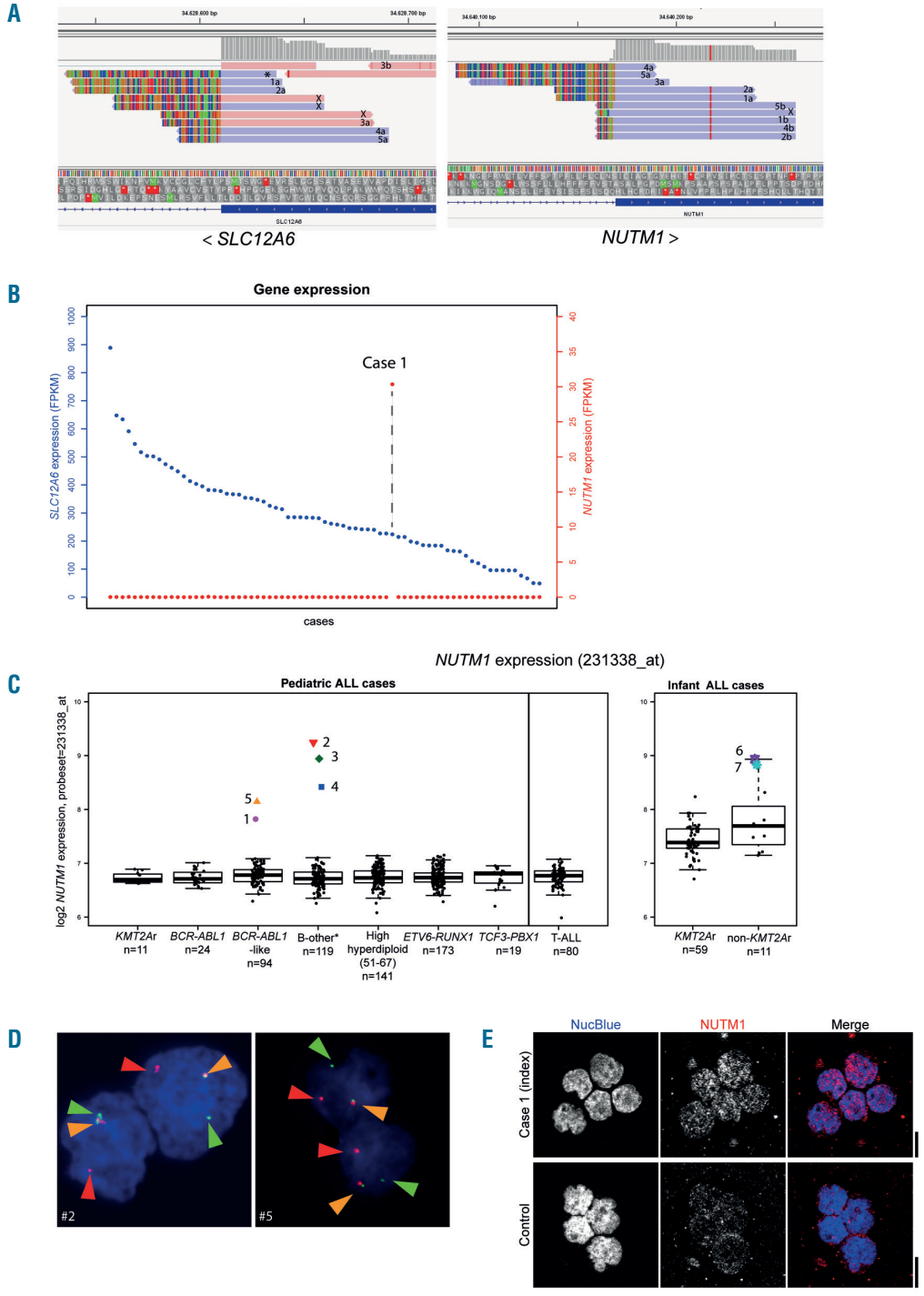


**Figure 1. *NUTM1* fusion identification.** (A) Chimeric total RNA sequencing reads of case #1 (*SLC12A6-NUTM1* fusion case; index case) aligned with STAR and visualized with the Integrative Genomic Viewer (version 2.4.10). The bright colors (red, brown, blue, green) show mismatches with the reference genome version hg19. The left panel shows chimeric reads mapped to *SLC12A6* exon 2, the right panel shows chimeric reads mapped to *NUTM1* exon 3. Matching numbers indicate that reads are from the same read pair, a and b indicate the two reads within a pair. *read maps to *NUTM1* exon 5, X read does not map to *NUTM1*. < and > show directions of *SLC12A6* and *NUTM1*. (B) Total RNA sequencing gene expression of *SLC12A6* (blue) and *NUTM1* (red) of all 71 cases of acute lymphoblastic leukemia (ALL), ordered on *SLC12A6* gene expression in fragments per kilobase per million. The dashed line connects *NUTM1* to *SLC12A6* in case 1 (*SLC12A6-NUTM1* fusion case; index case). (C) Boxplot showing the expression of *NUTM1* (probe set 231338_at) in 661 pediatric ALL cases and 70 infant ALL cases, divided per subtype. Outliers with *NUTM1* expression are displayed in color. Case #1 is our index case shown in panel (A), cases #2-#7 are additionally identified by expression of *NUTM1*. *B-other ALL: B-cell precursor ALL without one of the sentinel aberrations (excludes *KMT2A*-rearranged, *ETV6-RUNX1*, high hyperdiploid, *TCF3-PBX1*, *BCR-ABL1*, and *BCR-ABL1*-like). Within the non-*KMT2A*-rearranged (infant) cases there are seven B-other ALL cases. *KMT2Ar, KMT2A*-rearranged. (D) Representative examples of fluorescence *in situ* hybridization (FISH) of two cases with suspected *NUTM1* fusion. Orange arrows indicate a fusion signal, red arrows the break apart probe upstream of *NUTM1* and green arrows the break apart probe downstream of *NUTM1*. *Online Supplementary Figure S2* shows the FISH results of all studied cases. (E) Representative confocal microscope images of cytospins of the index case #1 with a *SLC12A6-NUTM1* fusion and a B-other ALL control sample immunostained with NUT antibody (NUTM1; red in merge). Cell nuclei were stained with NucBlue (blue in merge). Scale bars: 10 μm.

using the Cytocell *NUTM1* break-apart probe set MPH4800. Reverse transcriptase polymerase chain reaction (RT-PCR) was carried out using the primers shown in *Online Supplementary Table S1*. Immunofluorescence staining was performed using NUT antibody C52B1 (#3625, Cell Signaling Technology). Methods are described in more detail in the *Online Supplement*.

RNA sequencing analysis revealed an in-frame *SLC12A6-NUTM1* fusion transcript composed of exons 1-2 of *SLC12A6* fused to exons 3-8 of *NUTM1*, encoding almost the complete coding region of *NUTM1* (Figure 1A, *Online Supplementary Figure S1*). This fusion was confirmed by RT-PCR and Sanger sequencing (Table 1, *Online Supplementary Table S2*). Both genes are located on 15q14 within 5.3 kb distance on opposite strands, and the fusion could result from an inversion. The fusion transcript is predicted to encode a chimeric protein, likely containing an acidic binding domain for the histone acetyltransferase EP300 from NUTM1.[3] The *SLC12A6-NUTM1* fusion case showed expression of *SLC12A6* in the same range as the other BCP-ALL cases, while *NUTM1* expression was high in the *SLC12A6-NUTM1*

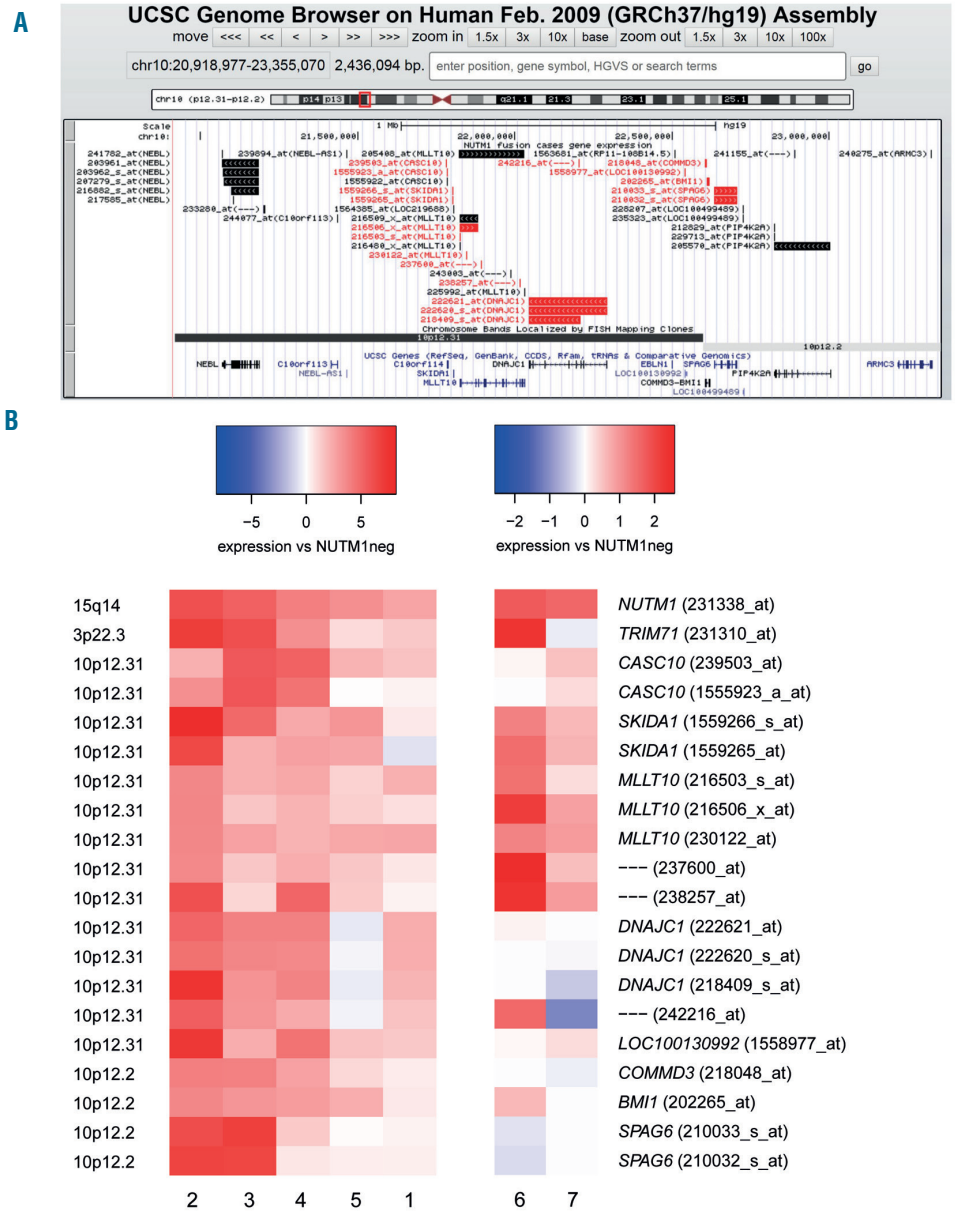


**Figure 2. Gene expression on chromosome band 10p12.31-12.2 in *NUTM1* fusion cases.** (A) Visualization of all probe sets within the 10p12.31-12.2 chromosome band. UCSC genome browser view of chromosome location (first track), probe sets (second track), chromosome band (third track), and UCSC genes (fourth track) aligned to GRCh37/hg19. In the second track, all probe sets that map to the location in this view are visualized. Each probe set is visualized with a thick band from start to end and arrows indicating the strand. A black band means no different expression between *NUTM1*-positive and *NUTM1*-negative cases, red means increased expression in *NUTM1*-positive cases *versus* *NUTM1*-negative cases (false discovery rate ≤0.01). (B) Heatmap of the expression of *NUTM1*, *TRIM71*, and 10p12.31-12.2 upregulated genes in *NUTM1*-positive *versus* *NUTM1*-negative cases (false discovery rate ≤0.01) in the pediatric population-based cohort. Expression of these genes is shown for the infant *NUTM1*-positive cases as well. Expression values are centered around 0 using the median of all B-other ALL and *NUTM1* fusion cases and scaled by 2x root-mean-square for the pediatric cohort and the infant cohort individually. Blue indicates reduced expression, red indicates increased expression compared with the median over all cases per cohort. Within the 10p12.31-12.2 chromosome band, genes are ordered by genomic location.

fusion case but absent in the remaining 70 BCP-ALL cases (Figure 1B, *Online Supplementary Figure S1*). NUTM1, previously known as NUT (nuclear protein in the testis), is involved in normal germ cell maturation. *NUTM1* is frequently fused to *BRD4* or *BRD3* in NUT midline carcinoma, a subtype of squamous cell cancer, and these fusions are associated with a block in differentiation.[4]

To identify additional *NUTM1* fusion cases, we studied the gene expression of *NUTM1* in a previously described cohort of 661 children with ALL[5] and a cohort of 70 infants with ALL.[6] We confirmed high expression of *NUTM1* in the *SLC12A6-NUTM1* fusion case (index case #1) and identified four additional pediatric and two infant BCP-ALL cases with high *NUTM1* expression (Figure 1C, Table 1). In both cohorts, reflecting all different cytogenetic subtypes, these cases were restricted to the B-other ALL subgroup without sentinel cytogenetic abnormalities (n=210 pediatric, n=7 infants). FISH with *NUTM1* break apart probes could be performed for four cases with high *NUTM1* expression for which cytospins were available. All four cases (three pediatric and one infant) showed a FISH break apart pattern suggesting a balanced translocation (Figure 1D, *Online Supplementary Figure S2*). The index case #1 showed no FISH break apart signal, in line with a small inversion of the region between the FISH probes. RT-PCR followed by Sanger sequencing and/or RNA sequencing revealed *CUX1-NUTM1* fusions involving exons 5/4-8 of *NUTM1* in pediatric cases #2 and #3 respectively, an *IKZF1-NUTM1* fusion involving exons 5-8 of *NUTM1* in pediatric case #4, and an *ACIN1-NUTM1* fusion involving exons 3-8 of *NUTM1* in infant case #7 (Table 1; *Online Supplementary Table S2*). Moreover, using a NUTM1 antibody, we detected nuclear staining in our index case #1 harboring a *SLC12A6-NUTM1* fusion (Figure 1E). We conclude that *NUTM1* is normally not expressed in leukemic lymphoblasts and that its high level of expression in our seven patients results from a gene fusion.

Our combined results showed that *NUTM1* fusions occurred in 5/210 (2.4%) of pediatric and in 2/7 of infant BCP-ALL cases without a sentinel cytogenetic aberration, and that *NUTM1* has different fusion partners. Several single *NUTM1* fusions were previously reported in pediatric and infant BCP-ALL.[7–10] Recently, Li *et al*. defined a BCP-ALL expression-based subgroup in a large cohort enriched for *NUTM1* fusions.[11] Combining our results with the *NUTM1* fusions described in literature suggests that *NUTM1* fusions are a rare but recurrent event in pediatric BCP-ALL.

Among our seven *NUTM1*-positive cases no other recurrent deletions or mutations were detected using multiplex ligation-dependent probe amplification and a custom sequencing panel (Table 1). The recurrence of *NUTM1* aberrations in BCP-ALL cases without the presence of a known driver and the resulting expression of *NUTM1* suggests that *NUTM1* fusions could be an oncogenic driver in leukemia. Five out of seven patients with a *NUTM1* fusion were stratified into a standard-risk protocol and all seven patients are in long-term first continuous complete remission with a median follow-up time of 8.3 years (range, 4.8-13.8 years). The clinical outcomes suggest that *NUTM1* fusions in BCP-ALL have a favorable prognosis. The possibly good prognosis in BCP-ALL opposes the unfavorable prognosis associated with the *BRD4-NUTM1* fusion in NUT midline carcinoma; only one in 62 known patients was cured (reviewed by C.A. French).[4] The apparently good prognosis of *NUTM1* fusions in BCP-ALL might be due to a different role of the fusion partner or to the different cell type in which they occur.

To get an insight into the underlying biology, we compared gene expression between the five *NUTM1*-positive pediatric BCP-ALL cases and the remaining 112 *NUTM1*-negative B-other ALL [excluding *BCR-ABL1*-like and hypodiploid (≤39 chromosomes)] cases and identified 130 differentially expressed probe sets (false discovery rate ≤0.01; 116 upregulated and 14 downregulated) representing 80 unique genes (*Online Supplementary Table S3*). As expected, the most significant differentially expressed gene was *NUTM1* (3.5-fold upregulated). The highest upregulated gene was *TRIM71* (9.8-fold upregulated). Functional annotation showed enrichment of genes from chromosome bands 7p15-p14 (Bonferroni adjusted *P*-value=$9.25 \times 10^{-6}$; which harbors among others the *HOXA* gene cluster) and 10p12.31 (*P*=$4.05 \times 10^{-4}$). Visualization of the location of differentially expressed probe sets on chromosome 10 showed that the enrichment extended to a small part of 10p12.2 that harbors among others *BMI1* (Figure 2A). We visualized the expression of significantly differentially expressed probe sets located on 10p12.31-12.2 and 7p15-p14 in all seven *NUTM1*-positive cases (Figure 2B, *Online Supplementary Figure S3*). The genes on chromosome band 10p12.31-12.2 were variably upregulated in six of seven cases, whereas the *HOXA* cluster was upregulated in the two highest *NUTM1*-expressing pediatric cases (both *CUX1-NUTM1*) and the two infant cases (including one *ACIN1-NUTM1*). Interestingly, Li *et al*. showed *HOXA* overexpression restricted to the same *NUTM1* fusions, suggesting that upregulation of *HOXA* genes depends on the *NUTM1* fusion partner.[11] In our dataset, expression of the 10p12.31-12.2 and *HOXA* cluster genes seems to be positively correlated to *NUTM1* expression levels (*Online Supplementary Figure S4*). In the 10p12.31-12.2 region, expression of all genes represented on the Affymetrix U133 Plus 2 array (18 probe sets) was significantly increased in the *NUTM1*-positive cases (Figure 2A). In the 7p14-p15 region, expression of most but not all genes was significantly increased in the *NUTM1*-positive cases (*Online Supplementary Figure S3B*).

The NUTM1 protein is capable of binding and thereby stimulating the histone acetyltransferase activity of the EP300 protein.[3] Interestingly, a single nucleotide polymorphism in chromosome band 10p12.31-12.2, specifically in an enhancer region of *BMI1*, is associated with increased risk of BCP-ALL.[12] The EP300 protein preferentially binds the risk allele of *BMI1* and this binding is hypothesized to increase *BMI1* expression, resulting in leukemia via increased proliferation and reduced apoptosis.[12] *BMI1*, a proto-oncogene, enhances self-renewal of hematopoietic stem cells and is capable of converting *BCR-ABL1*-positive progenitor cells to acute lymphoblastic leukemia.[13,14] Hence, we postulate that NUTM1 fusion proteins contribute to leukemogenesis by stimulating EP300, leading to upregulation of *BMI1* and other 10p12.31-12.2 genes in BCP-ALL.

In conclusion, we showed that *NUTM1* rearrangement is a rare but recurrent and possible oncogenic driver event in BCP-ALL. These rearrangements seem to have a good prognosis, but this should be confirmed in larger series. The *NUTM1* fusions involve many partners, resulting in overexpression of the normally silent *NUTM1* gene, and are associated with upregulation of a cluster of genes on 10p12.31-12.2 including the leukemogenic *BMI1* gene.

*Femke M. Hormann,[1,2] Alex Q. Hoogkamer,[1,2] H. Berna Beverloo,[3] Aurélie Boeree,[1,2] Ilse Dingjan,[1,2] Moniek M. Wattel,[3] Ronald W. Stam,[1] Gabriele Escherich,[4] Rob Pieters,[1,5] Monique L. den Boer[1,2,5,6] and Judith M. Boer[1,2]*

*[1]Princess Máxima Center for Pediatric Oncology, Utrecht, the Netherlands; [2]Oncode Institute, Utrecht, the Netherlands; [3]Department of Clinical Genetics, Erasmus Medical Center, Rotterdam, the Netherlands; [4]COALL – German Cooperative Study Group for Childhood Acute Lymphoblastic Leukemia, Hamburg, Germany; [5]DCOG – Dutch Childhood Oncology Group, Utrecht, the Netherlands and [6]Department of Pediatric Oncology and Hematology, Erasmus Medical Center - Sophia Children's Hospital, Rotterdam, the Netherlands*

*Funding: this work was supported by the Foundation Pediatric Oncology Center Rotterdam (SKOCR), the Dutch Cancer Society grant KWF-10482, and the KiKa Foundation Kika-264 grant.*

*Correspondence: JUDITH M. BOER.*
*j.m.boer-20@prinsesmaximacentrum.nl*
*doi:10.3324/haematol.2018.206961*

*Information on authorship, contributions, and financial & other disclosures was provided by the authors and is available with the online version of this article at www.haematologica.org.*

## References

1. Schwab C, Harrison CJ. Advances in B-cell precursor acute lymphoblastic leukemia genomics. HemaSphere. 2018;111(5):1.
2. Den Boer ML, van Slegtenhorst M, De Menezes RX, et al. A subtype of childhood acute lymphoblastic leukaemia with poor treatment outcome: a genome-wide classification study. Lancet Oncol. 2009;10(2):125–134.
3. Reynoird N, Schwartz BE, Delvecchio M, et al. Oncogenesis by sequestration of CBP/p300 in transcriptionally inactive hyperacetylated chromatin domains. EMBO J. 2010;29(17):2943–2952.
4. French CA. Pathogenesis of NUT midline carcinoma. Annu Rev Pathol. 2012;7(1):247–265.
5. van der Veer A, Waanders E, Pieters R, et al. Independent prognostic value of BCR-ABL1-like signature and IKZF1 deletion, but not high CRLF2 expression, in children with B-cell precursor ALL. Blood. 2013;122(15):2622–2629.
6. Stam RW, Schneider P, Hagelstein JAP, et al. Gene expression profiling-based dissection of MLL translocated and MLL germline acute lymphoblastic leukemia in infants. Blood. 2010;115(14):2835–2844.
7. Andersson AK, Ma J, Wang J, et al. The landscape of somatic mutations in infant MLL-rearranged acute lymphoblastic leukemias. Nat Genet. 2015;47(4):330–337.
8. Nordlund J, Bäcklin CL, Zachariadis V, et al. DNA methylation-based subtype prediction for pediatric acute lymphoblastic leukemia. Clin Epigenetics. 2015;7(1):11.
9. Marincevic-Zuniga Y, Dahlberg J, Nilsson S, et al. Transcriptome sequencing in pediatric acute lymphoblastic leukemia identifies fusion genes associated with distinct DNA methylation profiles. J Hematol Oncol. 2017;10(1):148.
10. Lilljebjörn H, Henningsson R, Hyrenius-Wittsten A, et al. Identification of ETV6-RUNX1-like and DUX4-rearranged subtypes in paediatric B-cell precursor acute lymphoblastic leukaemia. Nat Commun. 2016;7:11790.
11. Li J, Dai Y, Lilljebjörn H, et al. Transcriptional landscape of B cell precursor acute lymphoblastic leukemia based on an international study of 1,223 cases. Proc Natl Acad Sci U S A. 2018;115(50):E11711–E11720.
12. de Smith AJ, Walsh KM, Francis SS, et al. BMI1 enhancer polymorphism underlies chromosome 10p12.31 association with childhood acute lymphoblastic leukemia. Int J Cancer 2018;143(11):2647–2658.
13. Sengupta A, Ficker AM, Dunn SK, Madhu M, Cancelas JA. Bmi1 reprograms CML B-lymphoid progenitors to become B-ALL-initiating cells. Blood. 2012;119(2):494–502.
14. Rizo A, Dontje B, Vellenga E, Haan G De, Schuringa JJ. Long-term maintenance of human hematopoietic stem/progenitor cells by expression of BMI1. Blood. 2008;111(5):2621–2630.
15. Jerchel IS, Hoogkamer AQ, Ariës IM, et al. RAS pathway mutations as a predictive biomarker for treatment adaptation in pediatric B-cell precursor acute lymphoblastic leukemia. Leukemia. 2018;32(4):931–940.